Agricultural Science; Vol. 7, No. 2; 2025
ISSN 2690-5396 E-ISSN 2690-4799
https://doi.org/10.30560/as.v7n2p17

Design and Performance Testing of the Hydraulic System for the Pickup Assembly of a Residual Film Recovery Machine

Yapeng Li[1] & Nan Zang[1]

[1] School of Agricultural Engineering, Jiangsu University, Zhenjiang, Jiangsu, China

Correspondence: Yapeng Li, School of Agricultural Engineering, Jiangsu University, Zhenjiang, Jiangsu, China.

Received: November 1, 2025 Accepted: November 10, 2025 Online Published: November 14, 2025

Abstract

Addressing issues such as complex transmission structures and poor speed regulation in traditional mechanical residual film collectors used in Xinjiang cotton fields, this study designs a load-sensing hydraulic system for the pickup working components of residual film collectors. Field tests evaluated key parameters including operating pressure and flow rate, while investigating the influence of pickup chain speed and forward speed on residual film collection efficiency. Results indicate that the designed hydraulic system meets operational requirements under complex field conditions. When the forward speed varies between 0 and 12 km/h, the optimal pickup chain speed range is 57.6 to 83.6 r/min. This study provides theoretical basis and practical reference for optimizing hydraulic systems in residual film collectors.

Keywords: residual film collector, hydraulic system, load sensing, operational parameter optimization, field trial

1. Introduction

As a major cotton-producing region in China, Xinjiang began promoting plastic mulch technology in cotton fields during the 1980s. This technology significantly increased cotton yields and water resource utilization efficiency. However, the widespread use of plastic mulch has led to increasingly severe residual film pollution in farmland, creating so-called "white pollution"[1]. Residual plastic film disrupts soil structure, impairs crop growth, reduces agricultural productivity, and causes long-term harm to the agricultural ecosystem[2-3]. With the advancement of agricultural modernization, mechanized film residue recovery has become the primary method for addressing this pollution[4]. Currently, China's residual film collectors primarily employ chain-driven and drum-type designs, relying mainly on mechanical transmission. While these devices can perform automated functions such as film pickup, debris removal, and baling, they still suffer from low reliability, limited adaptability, and suboptimal recovery efficiency[5]. Particularly in the complex operational environment of Xinjiang cotton fields, traditional mechanical residual film collectors struggle to adjust pickup speeds in real-time according to field conditions, severely compromising recovery effectiveness.

Developed countries enforce stringent standards for agricultural film quality, predominantly using plastic mulch films with thicknesses exceeding 0.02 mm[6-7]. Overseas residual film collectors primarily employ roll-up designs, characterized by simple and efficient structures[8]. For instance, Sawyer[9] in the United States invented a film collector that significantly enhances recovery efficiency by synchronizing the forward speed of the implement with the rotational speed of the film roll. In hydraulic technology applications, R.L. Parish[10] designed a recovery device using a hydraulic motor to control the film roll speed, matching the roll's linear velocity to the working speed by adjusting the motor's rotation rate. This hydraulically driven roll-up design is widely adopted internationally.

China's residual film collectors primarily feature pickup-type combined operations, capable of simultaneously performing operations such as stalk cutting, film raking, and film collection. Based on differences in collection principles, they can be categorized into two main structural types: drum-type and chain-type. In recent years, domestic researchers have actively explored hydraulic technology applications for residual film collectors. Wang et al.[11] developed a hydraulic cotton field film collection and baling machine, optimizing operational parameters using a five-factor, three-level Box-Behnken design method. Li et al.[12-13] developed a hydraulic system for combined residual film pickup and stalk recovery machinery, enhancing bale formation success rates. Wang[14] designed an automatic contour-following hydraulic system for cotton stalk return and residual film recovery machinery, improving machine adaptability in complex environments.

Hydraulic technology finds increasingly widespread application in agricultural machinery, particularly in large-scale equipment like cotton pickers[15] and harvesters[16]. Load-sensing technology, a key development direction for hydraulic systems, automatically adjusts system output based on load variations, enhancing energy efficiency and system stability[17]. Threaded cartridge valve technology, characterized by compact structure and reliable performance, is gradually replacing traditional plate valves and stacked valves in modern agricultural machinery hydraulic systems[18-20]. The introduction of proportional control technology has transformed hydraulic control from traditional on-off operation to precise continuous proportional control, meeting the demands of high-pressure and high-flow applications[21-22]. Despite progress in residual film recovery machine research both domestically and internationally, the following issues persist: Insufficient depth in applying domestic hydraulic drive technology to residual film recovery machines, particularly limited research on pickup working components; Traditional mechanical residual film recovery machines struggle to achieve stepless adjustment of pickup speed, failing to adapt to complex and variable operating conditions; Existing research predominantly focuses on optimizing individual components or functions, lacking studies on coordinated control of the entire system; insufficient research exists on the quantitative relationship between operational parameters and recovery efficiency of residual film recovery machines.

To address the aforementioned issues, this paper investigates the hydraulic system design and control strategies for the pickup working components of residual film recovery machines. Key research areas include: designing a load-sensing hydraulic system for the pickup working components; validating system performance through field trials and analyzing the impact of operational parameters on recovery efficiency; establishing a matching relationship model between pickup chain speed and forward speed; and proposing an optimized control strategy to enhance the machine's adaptability and operational efficiency. This research holds significant importance for resolving technical challenges encountered during practical operations of residual film recovery machines, advancing the development of residual film recovery technology toward intelligent and efficient directions, and providing theoretical foundations and practical references for the technological upgrading and innovation of related equipment.

2. Hydraulic System Design for Residual Film Recovery Machines

2.1 System Design Requirements and Operating Condition Analysis

Residual film collectors operate in complex and variable environments. Xinjiang cotton fields feature diverse soil types, including sandy and clay soils, alongside uneven terrain and rocky areas, imposing stringent demands on the hydraulic system. Based on the structural characteristics of the 4MZ220D self-propelled residual film recovery machine, its film collection components primarily consist of a debris-cleaning auger assembly, a pickup chain assembly, and a film-rolling and baling assembly (Figure 1). The hydraulic system must meet the following design requirements: (1) Adaptability to complex operating conditions: The system must maintain stable operation despite variations in soil hardness, terrain undulations, and interference from residual crop straw. (2) Stepless speed adjustment: The pick-up chain speed must be continuously adjustable within 0-120 r/min to accommodate varying forward speeds (0-12 km/h). (3) Energy consumption and heat dissipation: System efficiency must exceed traditional mechanical transmission, with oil temperature controlled below 65°C to ensure long-term operational reliability. (4) Safety Protection: Incorporate safety measures such as relief valves and overload protection to prevent mechanism jamming or hydraulic shock damage to components. Based on field test data, the pick-up mechanism experiences significant torque fluctuations (0.003-703.412 N·m) during operation, with an average torque of 126.222 N·m. The system must demonstrate excellent load adaptability and dynamic response capability.

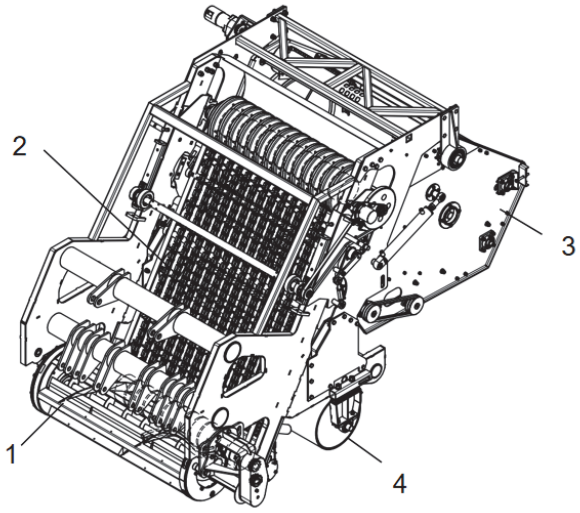

1. Debris-clearing auger assembly. 2. Pickup chain assembly. 3. Film-rolling baling assembly. 4. Ground roller.

Figure 1. Schematic diagram of the working component structure for residual film recovery

2.2 Load Analysis and Parameter Calculation of Working Components

2.2.1 Mechanical Model of the Pickup Mechanism

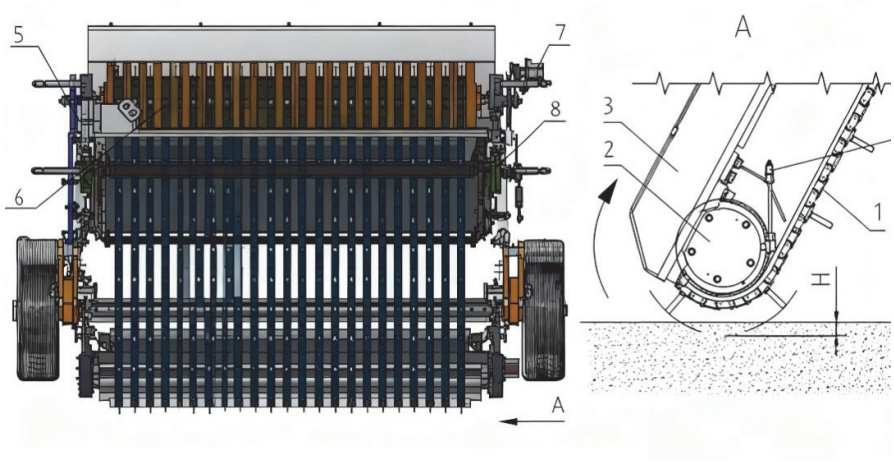

1. Pick-up Chain. 2. Idler Roller. 3. Frame. 4. Lubrication Port. 5. Hydraulic Motor. 6. Drive Roller. 7. Sensor. 8. Vibration Mechanism.

Figure 2. Schematic diagram of the working principle of the pickup chain

As shown in Figure 2, the pickup chain 1 is mounted on the drive roller 6 and driven roller 2. The frame 3 adjusts its tension. The drive roller, powered by the hydraulic motor mounted on the frame, drives the pickup chain to rotate. The frame 3 is suspended from the rear of the vehicle via a mechanism. The penetration depth H of the pickup tines is adjusted by regulating the depth-limiting wheel connected to the frame.

During operation, the pick-up chain primarily overcomes the tangential resistance between the pick-up teeth and the soil. Based on metal-soil dynamics research[23], the pick-up resistance is calculated using the following formula:

$$F_1 = \mu_1 BHlnv + f_\sigma \quad (1)$$

Where, F_1 represents the pickup resistance (N); μ_1 denotes the resistance coefficient between the pickup teeth and soil; B represents the number of pickup chain roots; H is the penetration depth of the pickup teeth into the soil (mm); v is the relative movement speed between the teeth and the ground surface (m/s); f_σ represents the frictional resistance (N).

The relationship between the linear speed of the pick-up tines (v) and the forward speed of the implement (v_m) is:

$$v = \frac{\pi D n}{60} + v_m \tag{2}$$

Where, v_m is the implement forward speed (m); D is the working diameter of the pick-up teeth (m); n is the rotational speed of the passive pick-up roller (r/min).

f_σ is the friction resistance between the pick-up mechanism and the soil (N):

$$f_\sigma = \mu_2 f_n \tag{3}$$

Where, μ_2 is the friction coefficient between the pick-up tines and the soil; f_n is the normal force exerted by the pick-up tines on the ground (N).

Torque formula for the drive roller to overcome pickup resistance:

$$T_1 = F_1 \times \frac{D}{2} = \left[\mu_1 BH \times ln\left(\frac{\pi D n}{60} + v_m\right) + \mu_2 f_n\right] \times \frac{D}{2} \tag{4}$$

In actual operation, the system must also overcome the resistance from the debris-clearing mechanism (T_1) and the resistance from its own mechanical structure (T_S). The total torque load is:

$$T_J = T_1 + T_S \tag{5}$$

Considering safety redundancy, the torque selection formula for the hydraulic motor is:

$$T = ikT_J \tag{6}$$

Where, i is the transmission ratio; k is the redundancy factor.

T_J cannot be directly calculated, thus requiring measurement of the actual load on the drive roller of the residual film recovery machine's pickup chain via a torque sensor.

2.2.2 Torque Characteristics Test Validation

To obtain authentic load data, field measurements of the pick-up roller torque were conducted using a TQ201 wireless torque sensor (Figure 3). Test conditions: Pickup roller speed 62 r/min, forward speed approximately 5 km/h. Results shown in Figure 4 indicate torque fluctuations ranging from 0.003 to 703.412 N·m, with an average of 126.222 N·m and a median of 62.999 N·m, demonstrating significant load variability.

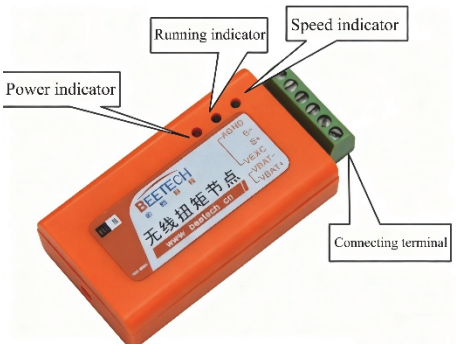

(a) TQ201 sensor

(b) Sensor mounting configuration on the pick-up roller

Figure 3. Torque node and pick-up roller

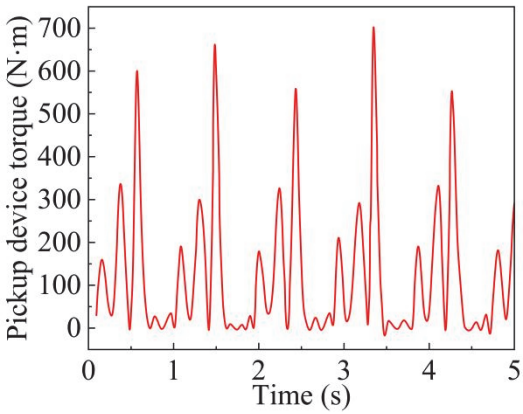

Figure 4. Torque waveform diagram of the pick-up device

Table 1. Loads during field operation of the pick-up roller

Pickup drive roller torque	Minimum	Maximum	Average	Median
Value (N·m)	0.003	703.412	126.222	62.999

The organized torque values are shown in Table 1. Substituting the maximum values measured by T_j ($T_{jmax} = 703$ N·m), the average values ($\overline{T_j} = 126$ N·m), and the values $i = 7/10$ and $k = 1.2$ into Equation (6) yields: $T_{max} = i(k \times T_J) = 590.5$ N·m and $\overline{T} = 106$ N·m.

Therefore, The Eaton 6K-390 cycloidal hydraulic motor is selected as the hydraulic motor for the pick-up chain. Its displacement is 390 cm³/r, torque is 1155 N·m, and maximum intermittent torque is 1635 N·m, meeting the requirements.

4.1 System Working Pressure and Flow Calculation

The system operating pressure depends on the maximum load torque. The torque-pressure relationship for the hydraulic motor is:

$$T = \frac{\Delta p V \eta}{20\pi} \tag{7}$$

Where, T represents the motor load (N·m); Δp denotes the pressure differential between the motor's inlet and outlet ports (bar); V indicates the motor displacement (cm³/r); η signifies the mechanical efficiency of the hydraulic motor, typically ranging from 80% to 95%.

$$\Delta p = p_1 - p_2 \tag{8}$$

$$p_1 = \frac{\mathrm{T}20\pi}{V\eta} + P_2 \tag{9}$$

Substituting $T = T_\varepsilon = 669$ N·m, $\eta = 0.8$, and $V = 390$ cm³/r into formula (8) yields $\Delta p = 135$ bar. Substituting $T = T_\varepsilon = 919$ N·m, $\eta = 0.8$, and $V = 390$ cm³/r into formula (8) yields $\Delta p_{max} = 185$ bar. Therefore, the system rated working pressure is set to 180 bar, with a maximum pressure of 305 bar.

System flow rate is calculated based on motor speed requirements:

$$q = \frac{Vn}{1000} \tag{10}$$

Where, n is the rotational speed of the hydraulic motor during operation (r/min).

The pick-up chain speed ranges from 0 to 120 r/min, corresponding to a flow rate of 0 to 46.8 L/min. Considering a leakage factor K=1.3, the maximum system flow requirement is 61 L/min.

2.3 Hydraulic Component Selection Calculation

2.3.1 Hydraulic Pump Selection

Maximum operating pressure of the hydraulic pump p_P:

$$p_P \geq p_1 + \sum \Delta p \tag{11}$$

Where, p_P is the maximum working pressure of the hydraulic pump (bar); p_1 is the maximum working pressure of the pick-up chain motor (bar); $\sum \Delta p$ is the total pipeline loss between the hydraulic pump outlet and the pick-up chain hydraulic motor inlet (bar).

Through load calculations, the maximum operating pressure of the pick-up chain motor is determined to be 185 bar, with other working loads estimated at 100 bar. The primary pressure loss in the piping system is attributed to the proportional flow valve, amounting to 20 bar. Consequently, the maximum operating pressure of the hydraulic pump should exceed 305 bar.

Determining the hydraulic pump flow rate and pressure q_{vmax}:

$$q_{vmax} \geq K \sum q_{vmax} \tag{12}$$

Where, K is the system leakage coefficient; $\sum q_{vmax}$ is the maximum flow rate of the pick-up chain hydraulic motor (L/min).

The maximum rotational speed of the pick-up chain motor is 120 r/min. Therefore, based on the hydraulic motor flow formula, the system flow rate is calculated as 46.8 L/min, with $K = 1.3$.

The maximum flow rate of the hydraulic pump should be greater than 61 L/min.

$$P = \frac{p_P q_{vP}}{\eta_P} \tag{13}$$

Where, p_P is the maximum operating pressure of the hydraulic pump (Pa); q_{vP} is the flow rate of the hydraulic pump (m^3/s); η_P is the overall efficiency of the hydraulic pump, typically 0.8 to 0.85 for a plunger pump.

Substituting $p_P = 305$ bar, $q_{vP} = 61$ L/min into Equation 13 and using $\eta_P = 0.8$ yields the maximum drive power $P = 38790$ W for the hydraulic pump. The Danfoss 45 series load-sensing pump (Figure 5) was selected, featuring a displacement of 45 cm^3/r, continuous operating pressure of 310 bar, and rated flow of 126 L/min (2900 r/min), meeting the requirements.

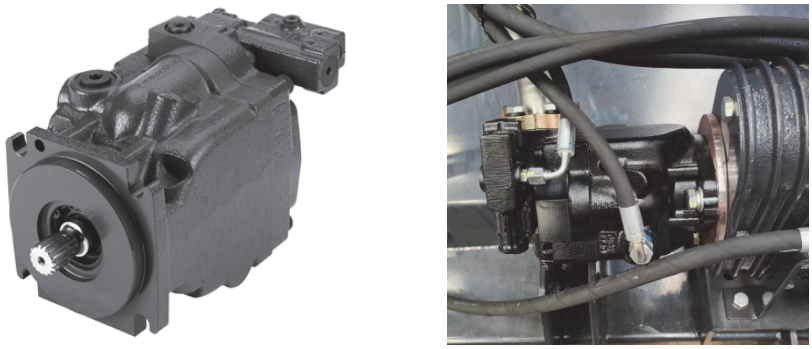

(a) Physical diagram (b) Installation diagram

Figure 5. Danfoss 45 series load-sensing pump

2.3.2 Actuator Selection

Based on the principle of equal flow in series circuits, the displacement of each motor is selected inversely proportional to its rotational speed:

$$q_1 = q_2 = q_3 \tag{14}$$

Where q is the flow rate through the hydraulic motor (L/min).

$$V_1 n_1 = V_2 n_2 = V_3 n_3 \tag{15}$$

Where the speed ratios for the picking chain, baler, and debris-cleaning auger are set at 1:0.8:1.2. The selection results are shown in Table 2, with physical diagrams depicted in Figure 6.

Table 2. Selection parameters of hydraulic motors

Hydraulic motor name	Model	Displacement (L/r)	Rated pressure (MPa)	Speed range (r/min)	Rated output torque (N·m)
Pickup chain motor	6K-390	390	20.5	0-387	930
Packing machine motor	2K-245	245	17	0-308	555
Debris removal auger motor	2K-195	195	17	0-385	465

The physical diagram of the motor and its installation position on the residual film machine are shown in Figure 6.

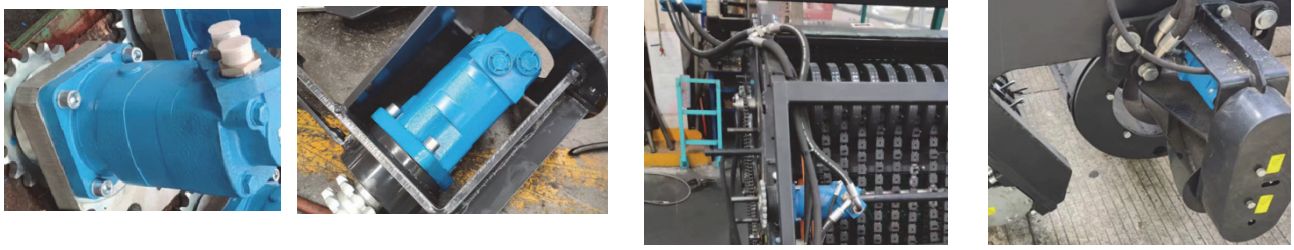

(a) 6K-390 Cycloidal Motor (b) 2K-195 Cycloidal Motor (c) Pickup chain and baler motor installation (d) Debris-cleaning auger motor installation

Figure 6. Hydraulic motor physical diagram

2.3.4 Selection of Auxiliary Components for the Hydraulic Motor

Accumulator: In this system, the accumulator primarily serves to absorb shocks. Its effective working volume is calculated using the formula:

$$V_0 = \frac{m}{2} v^2 \left(\frac{0.4}{p_0}\right) \left[\frac{10^3}{\left(\frac{p_2}{p_0}\right)^{0.285} - 1}\right] \tag{16}$$

Where, V_0 is the required accumulator volume (m^3); m is the total fluid mass in the pipeline (kg); v is the flow velocity in the pipe (m/s); p_2 is the minimum system operating pressure (bar); p_0 is the charging pressure (bar), set to 90% of the system operating pressure.

Assuming a system stable pressure of 170 bar and a maximum surge pressure of 305 bar,$m = 1$ kg, $v = 3$ m/s, the calculation yields $V_0 \approx 0.54$ L. Selects the GXQ-D-0.75-210-L diaphragm accumulator with a volume of 0.75 L.

Tank capacity: The empirical formula for tank volume is:

$$V = aq_v \tag{17}$$

Where, q_v is the volumetric flow rate of hydraulic oil discharged per minute by the pump (m^3/min); a is an empirical coefficient, typically ranging from 1 to 2 for mobile machinery.

Using empirical formula (17) with $a = 1.5$ and $q_v = 120$ L/min (maximum flow rate), the calculated value $V = 180$ L. Set to 200 L.

2.4 Descriptive Stats

2.4.1 Descriptive Stats

The hydraulic system model was established using AMESim software, as shown in Figure 7. Key parameters are listed in Table 3.

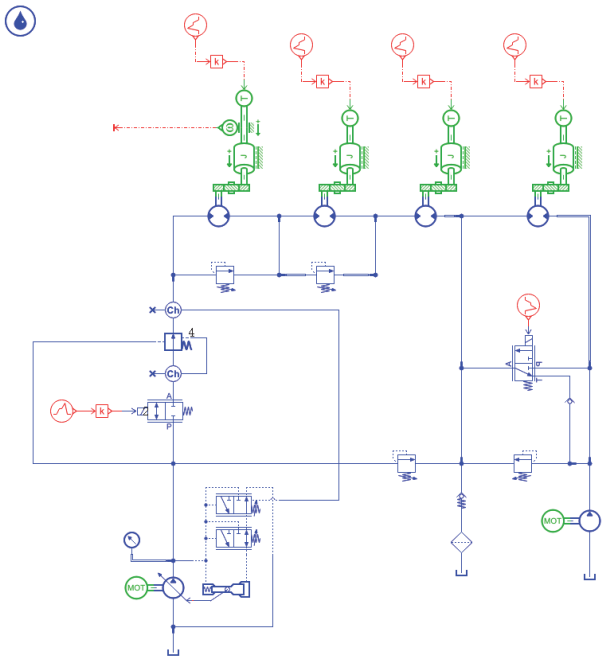

Figure 7. Simulation model

Table 3. Selection parameters of hydraulic motor

Component	Parameter	Description	Setting value
Film-forming chain motor	Motor displacement	Displacement (mL/r)	390
	Typical motor speed	Rotational speed (r/min)	1000
Rolling film motor	Motor displacement	Displacement (mL/r)	245
	Typical motor speed	Rotational speed (r/min)	1000
Cleaning motor	Motor displacement	Displacemen (mL/r)	195
	Typical motor speed	Rotational speed (r/min)	1000
Variable displacement pump	Pump displacement	Pump displacement (mL/r)	100
Power source	Shaft speed	Motor speed (r/min)	2250
Load-sensing valve	LS pilot differential pressure for maximum opening	LS set pressure (bar)	20
	Maximum controlled pressure	Maximum controlled pressure (bar)	230
Proportional flow valve	Valve rated current	Valve rated current (mA)	1800
Pressure compensating valve	Control pressure differential	Control pressure differential (bar)	7
	Pilot differential pressure for	Additional opening	1

	maximum closing	pressure due to spring stiffness (bar)	
Relief safety valve	Relief valve cracking pressure	Activation pressure (bar)	260

2.4.2 Standby Condition

When the residual film recovery machine is in standby mode, the hydraulic motor stops rotating. The proportional valve opening is zero, the pump maintains a standby pressure of 200 bar, and the flow rate is near zero. The simulation results for the standby condition are shown in Figure 8.

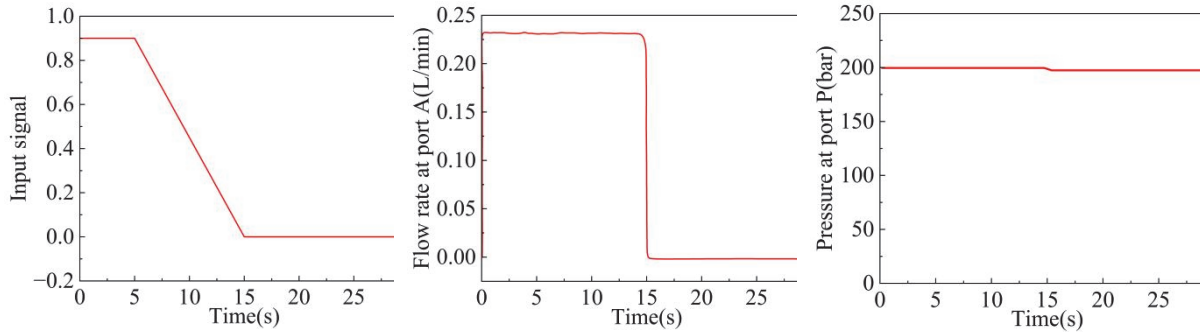

(a) Control signal simulation curve (b) Flow simulation curve (c) Pump outlet pressure simulation curve

Figure 8. Simulation curves of control signal, flow rate, and pump outlet pressure

2.4.3 Normal Operating Conditions

To simulate actual operating conditions, the load torque of the pick-up motor was varied between 300-600 N·m. System pressure fluctuated with load, but the proportional valve differential pressure remained stable (22±2 bar) with constant flow rate. The simulation curves for system pressure and differential pressure across the proportional valve are shown in Figure 9. The control signal input to the proportional valve during this period is depicted in Figure 10. Results indicate that system flow rate and the rotational speed of the pick-up roller hydraulic motor vary with the proportional valve opening, independent of the load on the pick-up working components.

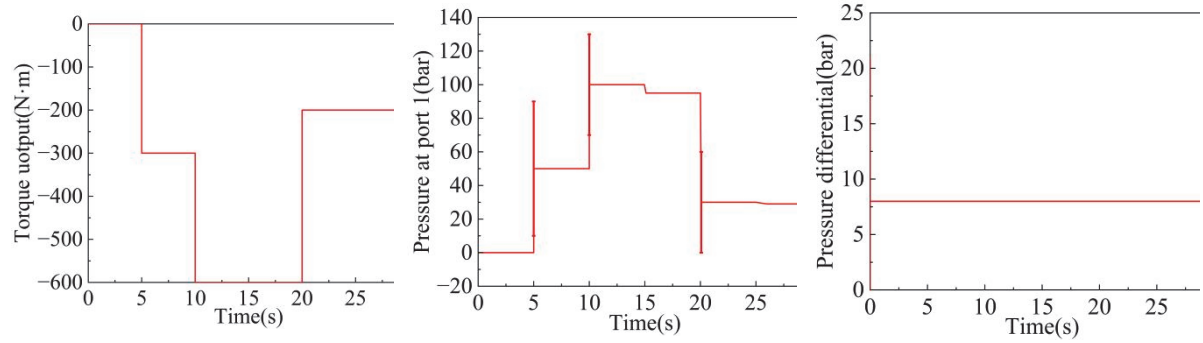

(a) Pickup motor load simulation curve (b) System pressure simulation curve (c) Simulation curve of proportional valve pressure differential

Figure 9. Simulation curves of load, pressure and pressure difference

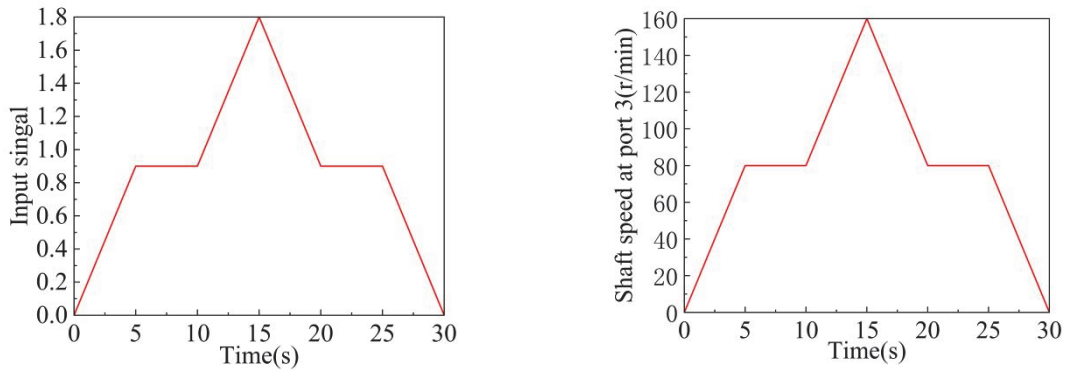

(a) Proportional valve control signal simulation curve

(b) Pickup roller hydraulic motor speed simulation curve

Figure 10. Simulation curves of control signal and motor speed

2.4.4 Blockage of Debris Removal Mechanism and Stoppage of Baler

Simulation results are shown in Figure 11. When the debris-cleaning motor overload occurs, the pump flow drops to zero, and the system pressure limits at 200 bar. When the baling mechanism stops rotating while the pick-up chain and debris-cleaning mechanism continue operating normally, the corresponding relief valve 10 for the baler's film-winding motor spills, as shown in Figure 12. Between 5s and 25s, the baler stops rotating while other actuators continue functioning normally. Based on the hydraulic simulation results, the selected circuit configuration is reasonable, the component selection is appropriate, and the designed hydraulic system for the pick-up chain can meet the operational requirements of the pick-up chain.

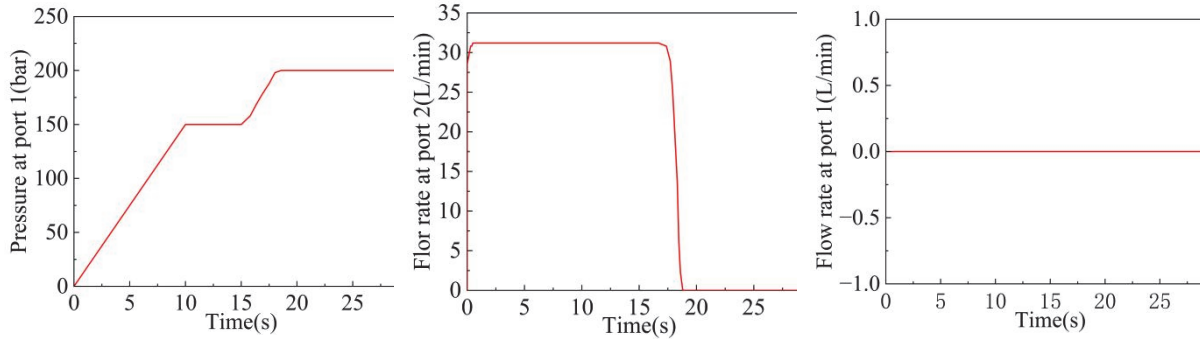

(a) System pressure simulation curve

(b) System flow simulation curve

(c) Relief valve flow simulation curve

Figure 11. Simulation curves of system pressure, system flow, and relief valve flow

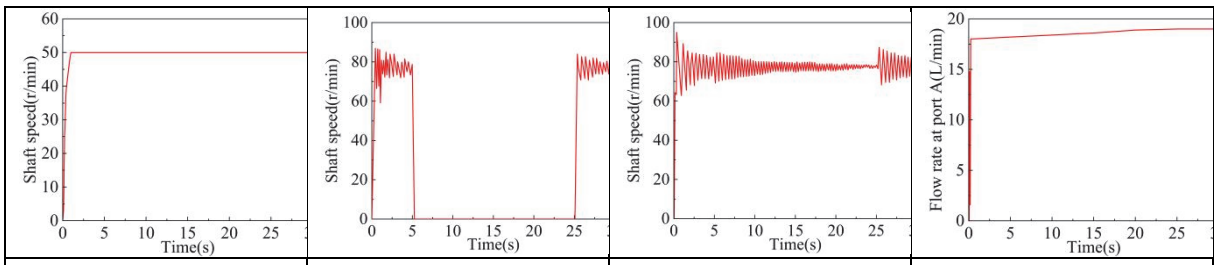

(a) Pickup motor speed	(b) Baling motor speed	(c) Debris removal auger motor speed	(d) System flow

Figure 12. Simulation curves of hydraulic system flow rate and motor speed

3. Hydraulic System Performance Testing and Parameter Optimization

3.1 Test Objectives and Conditions

The tests were conducted in November 2023 at Yingbositan Village, Kumish Town, Toksun County, Turpan City, Xinjiang. The area features sandy soil with 0.008 mm thick plastic film. The land is level but contains impurities such as stones and wooden stakes, presenting a complex operating environment. The tested model was an upgraded towed 4JMLQ-210 residual film collector equipped with a hydraulic system incorporating key components such as a load-sensing pump, proportional flow valve, and cycloidal hydraulic motor. The test design adhered to the following principles: (1) Systematic approach: Testing covered critical hydraulic parameters including pressure, flow rate, and temperature; (2) Comparability: Orthogonal experimental design was employed to control variables and ensure comparable results; (3) Repeatability: Each test group was repeated three times, with averages taken to minimize random errors; (4) Practicality: Test conditions simulated real-world operational scenarios, enabling direct application of results to production.

3.2 Hydraulic System Performance Testing

3.2.1 Test Platform and Equipment

The test platform is based on a modified 4JMLQ-210 model. Core components of the hydraulic system include: (1) Main pump: Danfoss 45 series load-sensing pump (JR-R-S45B-LS type), displacement 45 cm^3/r; (2) Actuators: Eaton 6K-390 cycloidal hydraulic motor (pickup chain drive), 2K-245 motor (baler drive), 2K-195 motor (debris-cleaning auger drive); (3) Control valve: ATLANTIC CE001034 proportional flow valve, maximum flow 100 L/min; (4) Auxiliary components: GXQ-D-0.75-210-L accumulator, 200L oil tank, plate heat exchanger.

Testing equipment includes: (1) Pressure sensor: PT-719 hydraulic pressure transmitter (range 0-400 bar, accuracy ±0.5%); (2) Data acquisition: YAV8AD Plus data acquisition card, sampling frequency 100Hz; (3) Temperature monitoring: Fluke 62MAX infrared thermometer (accuracy ±1°C) and mechanical tank thermometer; (4) Flow measurement: Turbine flowmeter (range 0-150L/min, accuracy ±1%).

3.2.2 Hydraulic System Pressure Testing

Under operating conditions of implement forward speed 8 km/h and pick-up chain speed 85 r/min, pressure monitoring was conducted at four key system measurement points: (1) Point P1: Pump outlet pressure (port P of valve block); (2) Point P2: Pick-up chain motor inlet pressure (LS feedback pressure); (3) Point P3: Inlet pressure of the baler motor; (4) Point P4: System return oil back pressure. Test results are shown in Figure 13, with statistical analysis of pressure data presented in Table 4.

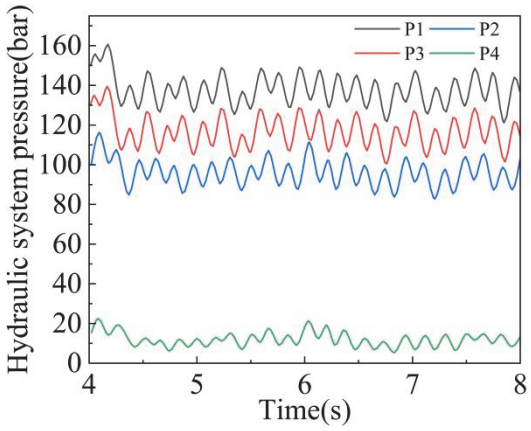

Figure 13. Hydraulic system pressure test waveform graph.

Table 4. Statistical analysis of hydraulic system pressure test results (unit: bar)

Test Point	Average	Standard Deviation	Maximum	Minimum	Fluctuation range
P1 (Pump outlet)	142.3	8.7	156.2	128.5	27.7

P2 (Pickup chain motor inlet)	120.1	6.3	132.4	113.2	19.2
P3 (Packing machine motor import)	85.6	3.2	90.1	82.3	7.8
P4 (System back pressure)	5.2	0.5	5.8	4.7	1.1

Key pressure differential analysis: (1) Proportional valve pressure differential $\Delta p1 = p1 - p2 = 22.2 \pm 2.4$ bar, indicating the load-sensing system maintains stable pressure differentials; (2) Pickup chain motor load pressure differential $\Delta p2 = p2 - p3 = 34.5 \pm 10.4$ bar, exhibiting significant fluctuations reflecting operational load variations; (3) Total load pressure differential $\Delta p3 = p3 - p4 = 80.4 \pm 3.1$ bar for the baler and debris-cleaning motor, which remains relatively stable. Compared to the hydraulic system studied by Li Jingkai et al. in Reference[20], this system exhibits a narrower pressure fluctuation range, demonstrating the superiority of load-sensing control.

3.2.3 System Flow Rate, Oil Temperature, and Stability

Flow rate test results indicate that the system achieves stepless speed regulation within the pick-up chain speed range of 0-120 r/min, with flow linearity error < 3%. Oil temperature test data are shown in Table 5.

Table 5. Hydraulic system temperature test results (unit: °C)

Test time	Ambient temperature	Tank temperature	Pump outlet temperature	Maximum motor housing temperature	Radiator outlet temperature
13:12 (No load)	9	12	15	18	8.5
14:30 (Homework 1h)	11	35	58	53	14.2
4:00 PM (Assignment 2.5 hours)	10	44	65.8	55	17.3
19:21 (Offline)	5	23	25	21	9.1

Regarding system stability, continuous operation for 4 hours without failure demonstrated superior temperature rise control compared to the hydraulic system studied by Wang Cheng et al.[19]. The maximum temperature of 65.8°C remained below the permissible value of 80°C. Under debris-jamming conditions in the cleaning mechanism, the relief valve promptly activated (Figure 14), maintaining system pressure within safe limits and validating the reliability of the system's protective function.

Figure 14. Overflow valve protection during mechanism jam

3.3 Comparison Test of Speed Control Methods for Pickup Chain Drive Rollers

3.3.1 Test Design and Evaluation Criteria

An orthogonal experimental design was employed to investigate the effects of pick-up chain speed (x_1) and forward speed (x_2) on residual film recovery efficiency. Evaluation metrics included:

Y_1, measured per GB/T 25412-2021 standard, calculated as:

$$Y_1 = \left(1 - \frac{W}{W_0}\right) \times 100\% \tag{18}$$

Where, Y_1 is the residual film pickup rate (%), W is the residual film mass after operation (g), and W_0 is the residual film mass before operation (g).

Formula for impurity rate (Y_2):

$$Y_2 = \left(1 - \frac{E}{E_0}\right) \times 100\% \tag{19}$$

Where, Y_2 is the impurity rate (%), E is the mass of pure residual film (kg), and E_0 is the total baled mass (kg).

The experimental factor level design is shown in Table 6. Based on preliminary tests, material accumulation occurred at rotational speeds below 65 r/min, while severe film leakage occurred above 95 r/min. Therefore, this range was set.

Table 6. Experimental factor coding table

No.	Experimental factor	
	Pickup speed x_1 (r/min)	forward speed x_2 (km/h)
1	65	1
2	75	2
3	85	3
4	95	4

3.3.2 Test Procedure and Data Acquisition

In accordance with GB/T 25412-2021, each test group was conducted within a 100m-long measurement zone using a five-point sampling method. Residual film was collected from depths of 0–100mm, washed, air-dried, and weighed using an electronic balance with 0.001g precision. A total of 16 test groups were performed in random order to minimize systematic errors. The measurement process is illustrated in Figures 15-16.

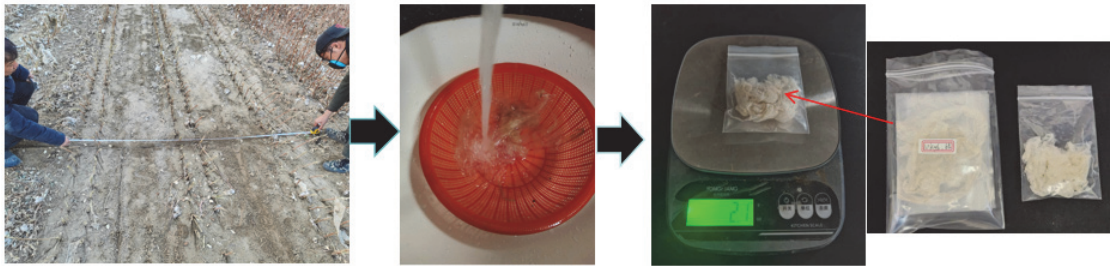

Figure 15. Collection and weighing of residual film post-operation

(a) Weighing before impurity separation (b) Weighing after impurity separation

Figure 16. Weighing of mulch film packaged by the residual film recycling machine

3.3.3 Experimental Results

Orthogonal test results are shown in Table 7. Data indicate a maximum purity rate of 87% (Test 3) and a minimum of 31% (Test 13); the lowest impurity rate was 68% (Test 16), while the highest reached 90% (Tests 9 and 10).

Table 7. Test protocols and results

No.	Factor 1	Factor 2	Picking efficiency Y_1 (%)	Impurity rate Y_2 (%)
1	1	1	83	86
2	1	2	85	86
3	1	3	87	85
4	1	4	81	84
5	2	1	69	86
6	2	2	80	85
7	2	3	87	85
8	2	4	85	87
9	3	1	65	90
10	3	2	69	90
11	3	3	84	85
12	3	4	81	84
13	4	1	31	74
14	4	2	49	74
15	4	3	58	74
16	4	4	55	68

3.4 Descriptive Stats

3.4.1 Experimental Results

Statistical analysis of experimental data was performed using SPSSAU software to evaluate the significant effects of various factors on the assessment indicators.

Single-factor ANOVA indicated (Table 8) that the picking chain speed had a highly significant effect on both the picking efficiency and the impurity rate ($p < 0.01$). The relationship between rotational speed and pickup rate is shown in Figure 17a, where the pickup rate decreases significantly as rotational speed increases. The relationship between rotational speed and impurity content is shown in Figure 17b, indicating significant differences in impurity content only at rotational speeds between 85 and 95.

Table 8. Results of single-factor ANOVA for pickup chain speed

Indicator	Factor	F value	p-value	Significance
Y_1	Rotational Speed	13.834	0.000	**
Y_2	Rotational Speed	35.553	0.000	**

Note: * indicates P < 0.05, ** indicates P < 0.01

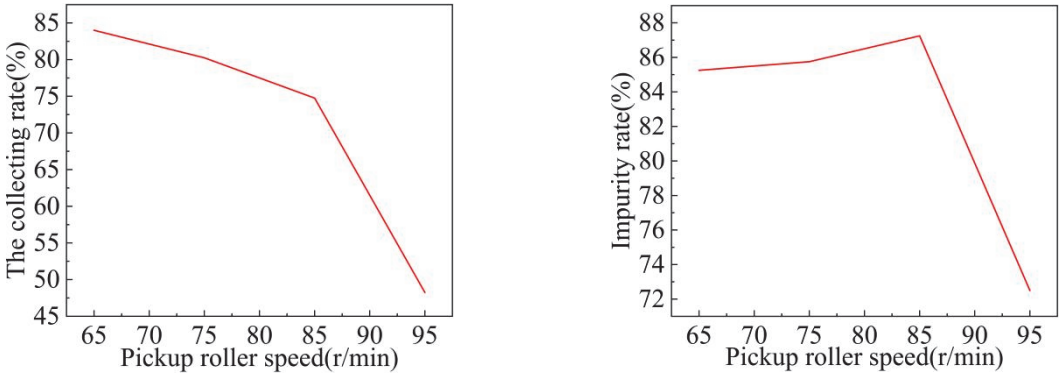

(a) Comparison of mean scores from ANOVA for picking chain speed and picking accuracy

(b) Comparison of mean scores from ANOVA for picking chain speed and impurity rate

Figure 17. Comparison of mean scores from ANOVA for picking chain speed versus picking rate and impurity rate

3.4.2 Effect of Forward Speed on Recovery Efficiency

Single-factor ANOVA indicates (Table 9) that forward speed has no significant effect on pickup rate ($p=0.534$). This means that within the speed range of 65 r/min to 95 r/min, samples exhibit no noticeable difference in pickup rate across varying forward speeds. However, mean scores (Figure 18a) suggest forward speed may positively influence pickup rate. Forward speed did not significantly affect contamination rate ($p=0.907$). Mean scores (Figure 18b) indicate no discernible variation in contamination rate across forward speeds.

Table 9. Results of single-factor ANOVA for forward speed

Indicator	Factor	F value	p-value	Significance
Y_1	Forward Speed	0.768	0.534	——
Y_2	Forward speed	0.182	0.907	——

Note: * indicates P < 0.05, ** indicates P < 0.01

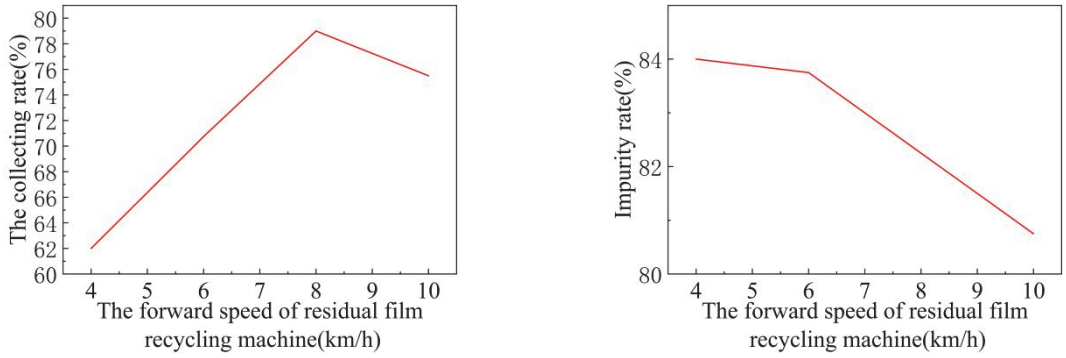

(a) Comparison of ANOVA mean scores for forward speed and pick rate

(b) Comparison of ANOVA mean scores for forward speed and impurity rate

Figure 18. Comparison of ANOVA mean scores for forward speed versus pick rate and impurity rate

3.4.3 Regression Model Developmen

Through multiple linear regression analysis, mathematical models were established for the relationship between operational parameters and evaluation indicators.

Pickup rate regression model:

$$Y_1 = 144.95 - 1.127x_1 + 2.438x_2 \quad (20)$$

Where, Y_1 represents pickup rate (%); x_1 denotes rotational speed (r/min); x_2 indicates forward speed (km/h).

The model's coefficient of determination R^2 is 0.747, indicating that rotational speed and forward speed together explain 74.7% of the variation in pickup rate. The model's F-test result is 19.182, with a p-value less than 0.05, confirming the model's statistical significance.

Contamination Rate Regression Model:

$$Y_2 = 116.025 - 0.367x_1 - 0.562x_2 \quad (21)$$

Where, Y_2 represents the contamination rate (%).

Model R^2=0.472, F=5.819, p=0.016, indicating significant but low explanatory power. Regression coefficient tests show (Table 10) that x_1 significantly affects both Y_1 and Y_2, while x_2 only significantly affects Y_1.

In summary, the rotational speed of the pick-up chain drive roller is the key factor influencing changes in pick-up efficiency and contamination rate. Forward speed significantly affects pick-up efficiency, and a linear relationship exists between forward speed and pick-up chain drive roller rotational speed.

Table 10. Significance test of regression coefficients

Model	Factor	Regression Coefficient	t-value	p-value	Significance
Y_1	Constant term	144.95	5.832	0.000	**
	x_1	-1.127	-5.685	0.000	**
	x_2	2.438	2.458	0.029	*
Y_1	Constant term	116.025	4.126	0.001	**
	x_1	-0.367	-3.262	0.006	**
	x_2	-0.562	-0.999	0.336	——

Note: * indicates P < 0.05, ** indicates P < 0.01

3.5 Establishment of the Recovery Rate Parameter Formula for Residual Film Recovery Machines

Based on regression analysis results, using the 80% pickup efficiency required by GB/T 25412-2021 as the standard, substitute $Y_1 = 80\%$ into Equation 3.4 to derive the relationship formula between forward speed and pickup chain rotation speed:

$$x_1 = \left(64.95 + 2.438x_2\right)/1.127 \quad (22)$$

The optimal picking chain speed at different forward speeds was calculated (Table 11). When x_2 equals 0 to 12 km/h, x_1 equals 57.6 to 83.6 r/min, ensuring optimal operational performance within this range.

Table 11. Recommended operating parameter matching table

x_1 (km/h)	4	6	8	10	12
x_2 (r/min)	66.3	70.6	74.9	79.3	83.6

Comparing the results of this study with the literature (Table 12) shows that the parameter optimization method proposed in this paper is more systematic. The recommended rotational speed range is consistent with the findings of Wang[19] (60–85 r/min), but this paper provides precise mathematical relationships through regression models.

Table 12. Comparison with related studies

Researcher	Model	Recommended speed range (r/min)	Research method	Pickup efficiency (%)
Wang et al.[19]	Hydraulic recovery machine	60–85	Box-Behnken design	78-85
Li et al.[20]	Combined operation machine	65-80	Orthogonal test	80-87
This study	4JMLQ-210	57.6–83.6	Orthogonal test and regression analysis	80-87

4. Conclusion

4.1 Research Summary

This study systematically investigated the hydraulic system design and control strategy for the pickup components of residual film recovery machines, addressing the practical needs of residual film recovery operations in Xinjiang cotton fields. Key findings include: (1) A load-sensing hydraulic system suitable for residual film collectors was designed. Theoretical calculations and field tests validated an operating pressure of 180 bar and maximum flow rate of 61 L/min, meeting operational demands under complex conditions. Compared to traditional mechanical transmission systems, the hydraulic system demonstrated significant advantages in speed regulation range, response speed, and operational stability. (2) Torque testing revealed the actual load characteristics of the pickup working components. Results indicated substantial torque fluctuations (0.003-703.412 N·m) in the drive roller of the pickup chain, with an average torque of 126.222 N·m. This data provides crucial reference for hydraulic component selection and system parameter optimization. (3) Orthogonal experimental design was employed to systematically investigate the impact of operational parameters on residual film recovery efficiency. A regression model was established linking the pickup chain rotational speed (x_1) and forward speed (x_2) to the pickup efficiency (Y_1). (4) Based on national standard requirements (pickup efficiency ≥80%), a formula was derived to determine the optimal matching relationship between forward speed and pickup chain rotational speed. The findings not only provide theoretical foundations and practical guidance for upgrading residual film recovery machinery but also offer reference methods and insights for optimizing hydraulic systems in agricultural machinery. As agricultural modernization advances, intelligent and efficient residual film recovery technologies based on hydraulic transmission will play an increasingly vital role in addressing "white pollution" in farmlands and promoting sustainable agricultural development.

4.2 Innovations and Contributions

The innovations and primary contributions of this study are reflected in the following aspects: (1) Hydraulic system design innovation: Load-sensing technology was applied to the hydraulic system of the residual film recovery machine. The post-valve pressure compensation (LUDV) technique resolved the flow distribution issue among multiple actuators. Compared to the system studied by Li et al.[20], this system achieved approximately 15% improvement in pressure stability. (2) Innovative parameter optimization method: A quantitative relationship model between operational parameters and recovery efficiency was established using regression analysis. Compared to the Box-Behnken design method employed by Wang et al.[19], this approach is more suitable for optimizing multi-factor, nonlinear agricultural machinery operational parameters. (3) Outstanding Practical Value: The research findings directly guide the operational parameter settings for plastic film recovery machines, providing technical support for enhancing recovery efficiency and reducing energy consumption. Table 13 compares the operational effectiveness of the recommended parameters with traditional methods.

Table 13. Comparison analysis of task effectiveness

Evaluation metrics	Traditional method	Recommended parameters in this study	Change range
Pickup efficiency (%)	70-75	80-87	Increase by 15-20%
Impurity rate (%)	15-20	12-16	Reduced by 20%
Energy consumption (kWh/hm²)	8.5-9.2	7.2-7.8	15% reduction

4.3 Research Limitations

Although this study achieved certain results, the following limitations remain: (1) Experimental conditions: The research was conducted solely in the Turpan region of Xinjiang. While this area is representative, the system's adaptability under different soil types and climatic conditions requires further validation. (2) Limited parameter range: The pickup chain rotational speed study was confined to 65-95 r/min, neglecting operational performance at lower or higher speeds, potentially overlooking more optimal operating points. (3) Simplified control strategy: This research primarily focused on hydraulic system design and parameter optimization, without exploring the application effectiveness of advanced control algorithms (e.g., fuzzy PID, adaptive control) within the system.

4.4 Research Prospects

Based on the findings and limitations of this study, future research may explore the following directions: (1) Intelligent control strategy research: Integrating modern control theory to investigate the application of intelligent algorithms like fuzzy control and neural networks in the hydraulic system of residue film collectors, enhancing the system's adaptive capabilities. (2) Multi-condition adaptability research: Further validating and optimizing system parameters under different soil types and crop residue levels to improve the equipment's versatility and adaptability. (3) Energy consumption optimization: Conduct in-depth analysis of the system's energy consumption characteristics. Implement measures such as pump control technology and energy recovery to further reduce operational energy consumption and improve economic efficiency. (4) System integration and validation: Apply research findings to the development of a new generation of residual film recovery machines. Conduct large-scale field trials to validate the system's reliability and practicality.

References

[1] Shi, Y. Q., Wang, Q., Dong, D., et al. (2023). Pollution status and impact of microplastics in Xinjiang cotton fields and its treatment techniques. *China Cotton*, *50*(9), 27–34.

[2] Sun, X., Gou, Y. R., Yan, H., et al. (2024). Microplastic pollution and distribution characteristics in a typical cotton field in northern Xinjiang, China. *Journal of Agro-Environment Science*, *43*(3), 571–580.

[3] Hua, Z. Y., Li, X., Jiang, N., et al. (2023). Occurrence characteristics and correlation of soil residual film in the main cotton producing areas of Xinjiang. *Xinjiang Agricultural Sciences*, *60*(12), 2932–2939.

[4] Chen, X. G. (2019). Technological innovation opens up a new chapter in agricultural mechanization. *China Rural Science & Technology,* (5), 30–35.

[5] Li, D., Zhao, W. Y., Xin, S. L., et al. (2020). Current situation and prospect of recycling technology of farmland residual film. *Journal of Chinese Agricultural Mechanization*, *41*(5), 204–209.

[6] Hu, Y., Liu, D. L., Wang, L., et al. (2019). The use and recycling experience of agricultural film in developed

countries. *World Agriculture,* (2), 89–94.

[7] Hao, F., Li, T., Han, Z., et al. (2019). Design and experiment of 11CH160 type residual film recovery machine [Paper presentation]. ASABE Annual International Meeting, St. Joseph, MI, United States.

[8] Guo, W., Wang, X., Lu, B., et al. (2019). Design and experiment of rotary nail tooth type residual plastic mulch recycling machine [Paper presentation]. ASABE Annual International Meeting, St. Joseph, MI, United States.

[9] Sawyer, A. G., & Roberson, R. L. (1993). *Plastic sheet take-up implement* (U.S. Patent No. 5,236,051). U.S. Patent and Trademark Office.

[10] Parish, R. L. (1999). An automated machine for removal of plastic mulch. *Transactions of the ASAE*, *42*(1), 49.

[11] Wang, C., Song, Y. H., Yang, J. M., et al. (2022). Design and parameter optimization of hydraulic baling machine for cotton field film recycling. *Journal of Chinese Agricultural Mechanization*, *43*(9), 30–39.

[12] Li, J. K., Wang, M., Lu, Y. T., et al. (2022). Design and experiment of hydraulic control system of 4MKJ plastic film recovery combined operation machine. *Journal of Agricultural Mechanization Research*, *44*(9), 160–167.

[13] Li, J. K., Wang, M., Wang, J. L., et al. (2022). Design and test of open type hydraulic system of 4MKJ plastic film recovery combined operation machine based on AMESim. *Journal of Chinese Agricultural Mechanization*, *43*(2), 43–49.

[14] Wang, J. W., Yang, H. M., Jiang, Y. X., et al. (2024). Design and test of automatic copying system for residual film recovery machine. *Journal of Chinese Agricultural Mechanization*, *45*(3), 44–50.

[15] Ke, C. P., & Ding, W. S. (2021). Design and AMESim simulation analysis of hydraulic system for double-row three-line cotton picker. *Jiangsu Agricultural Sciences*, *49*(11), 170–177.

[16] Wang, H., Shu, C. X., Liao, Q. X., et al. (2017). Design and test of series-parallel combined hydraulic drive system for rapeseed combine harvester. *Journal of Huazhong Agricultural University*, *36*(5), 90–98.

[17] Chen, S. Y., Zhao, J. J., Mao, E. R., et al. (2017). Structural modeling and performance analysis of load-sensing variable pump. *Transactions of the Chinese Society of Agricultural Engineering*, *33*(3), 40–49.

[18] Fang, S. G. (1987). Application of two-way cartridge valve. *Tractor & Farm Transporter*(1), 22–25.

[19] Xie, B., & Mao, E. R. (2006). Development of CAN intelligent nodes of tractor electronic hydraulic hitch system. *Transactions of the Chinese Society for Agricultural Machinery*, *37*(12), 1–3+16.

[20] Li, Y. T. (2023). Application and development prospect of hydraulic transmission technology in harvesting machinery. *Contemporary Farm Machinery,* (3), 65–66.

[21] Xu, Y. Z. (2013). *Hydraulic screw cartridge valve technology and applications*. China Machine Press.

[22] Zhang, H. P. (2012). *Hydraulic screw cartridge valves*. China Machine Press.

[23] Yao, Y. S., & Zeng, D. C. (1988). Study on the relationship between metal-soil friction resistance and sliding speed. *Transactions of the Chinese Society for Agricultural Machinery,* (4), 33–40.